showing that bonding capabilities of silylene, germylene, and stannylene are considerably lower than those of methylene.

The electronic states $^7B_1$, corresponding to species with a formal σ bond, lie above the $^5B_1$ states, and the $^5B_1$-$^7B_1$ splitting diminishes regularly down the group. With the exception of $MoCH_2$, the septets $^7B_1$ are first-order stationary points with an imaginary frequency associated with a wagging displacement of hydrogen atoms out of the molecular plane. Full optimization of these species leads to C_s structures (states $^7A'$) considerably distorted from planarity. This anomalous behavior of the transition metal-metal bond increases down the group and is related to nonclassical distortions observed in the series of compounds Si_2H_6, Ge_2H_6, and Sn_2H_6. Because of such distortion, the ground state of the heaviest element of the series, $MoSnH_2$, is found to be bent (C_s, state $^7A'$) instead of planar (C_{2v}, state $^5B_1$).

Finally, comparison of naked $MoM'H_2$, with their pentacarbonylated homologous $(CO)_5Mo{=}M'H_2$, reveals that, as far as Mo-M' bond strengths and dissociation energies are concerned, the Fischer-type of complexation is stronger than the Schrock one.

Note Added in Proof. After this paper was submitted for publication, we found out the work reported by Cundari and Gordon[28] on the nature of the transition-metal-silicon double bond in which geometries and force constants of charged species $CrM'H_2^+$ (M' = Si, Ge, and Sn) were also reported. The results and trends observed are in agreement with those found in the present work.

Acknowledgment. This work was supported the Dirección General de Investigación Científica y Técnica of Spain, Project No. PB89-0561.

Supplementary Material Available. Mulliken population analysis for all states of $MoM'H_2$ complexes are only available on request from the author (11 tables).

(28) Cundary, T. R.; Gordon, M. S. *J. Phys. Chem.* **1992**, *96*, 631.

UFF, a Full Periodic Table Force Field for Molecular Mechanics and Molecular Dynamics Simulations

A. K. Rappé,* C. J. Casewit,‡ K. S. Colwell, W. A. Goddard III,# and W. M. Skiff†

Contribution from the Department of Chemistry, Colorado State University, Fort Collins, Colorado 80523. *Received March 23, 1992*

Abstract: A new molecular mechanics force field, the Universal force field (UFF), is described wherein the force field parameters are estimated using general rules based only on the element, its hybridization, and its connectivity. The force field functional forms, parameters, and generating formulas for the full periodic table are presented.

I. Introduction

Parameters and functional forms are the vital infrastructure of molecular mechanics and dynamics force fields. One of the most important uses of molecular dynamics and energy minimization is the estimation of structures for new molecules. Unfortunately, the popular force fields, based on the classic work in the field,[1a-z] are limited to particular combinations of atoms, for example, those of proteins, organics, or nucleic acids.[1aa-ff] Progress has been made toward development of force fields which could, in principle, be extended to the entire periodic table though systematic procedures for obtaining the parameters have not been presented.[2,3] Further, the angle bend function used in these standard force fields (harmonic in θ) has the wrong shape to describe angular distortion approaching 180° for a nonlinear molecule. This functional form cannot describe the dynamics of inorganic materials such as zeolites which have equilibrium angles of ~150° and distort thermally to 180° with barriers to inversion of ~1 kcal/mol.[4a] In order to facilitate studies of a variety of atomic associations, we have developed a new force field using general rules for estimating force field parameters based on simple relations. This set of fundamental parameters is based only on the element, its hybridization, and connectivity. We refer to this new force field as a Universal force field (UFF). The angular distortion functional forms in UFF are chosen to be physically reasonable for large amplitude displacements. The force field functional forms and parameters are discussed in section II. Results for select organic, main group inorganic, and transition metal complex structures are provided in section III. Reference compounds used to obtain covalent radii for the elements are

‡Calleo Scientific, 1300 Miramont Dr., Fort Collins, CO 80524.
Materials and Molecular Simulation Center, Beckman Institute, California Institute of Technology, Pasadena, CA 91125.
†Shell Development Co., Westhollow Research Center, 3333 Hwy. Six South, Houston, TX 77082.

(1) (a) Bixon, M.; Lifson, S. *Tetrahedron* **1967**, *23*, 769. (b) Lifson, S. *J. Chim. Phys. Physicochim. Biol.* **1968**, *65*, 40. (c) Lifson, S.; Warshel, A. *J. Chem. Phys.* **1968**, *49*, 5116. (d) Levitt, M.; Lifson, S. *J. Mol. Biol.* **1969**, *46*, 269. (e) Warshel, A.; Levitt, M.; Lifson, S. *J. Mol. Spectrosc.* **1970**, *33*, 84. (f) Warshel, A.; Lifson, S. *J. Chem. Phys.* **1970**, *53*, 582. (g) Altona, C.; Sundaralingam, M. *Tetrahedron* **1970**, *26*, 925. (h) Altona, C.; Sundaralingam, M. *J. Am. Chem. Soc.* **1970**, *92*, 1995. (i) Altona, C.; Hirschmann, H. *Tetrahedron* **1970**, *26*, 2173. (j) Warshel, A. *J. Chem. Phys.* **1971**, *55*, 3327. (k) Bartell, L. S.; Burgi, H. B. *J. Am. Chem. Soc.* **1972**, *94*, 5239. (l) Warshel, A. *Isr. J. Chem.* **1973**, *11*, 709. (m) Ermer, O.; Lifson, S. *J. Am. Chem. Soc.* **1973**, *95*, 4121. (n) Bartell, L. S.; Plato, V. *J. Am. Chem. Soc.* **1973**, *95*, 3097. (o) Ermer, O. *Tetrahedron* **1974**, *30*, 3103. (p) Ermer, O.; Lifson, S. *J. Mol. Spectrosc.* **1974**, *51*, 261. (q) Hagler, A. T.; Lifson, S. *Acta Crystallogr., Sect. B* **1974**, *30*, 1336. (r) Hagler, A. T.; Huler, E.; Lifson, S. *J. Am. Chem. Soc.* **1974**, *96*, 5319. (s) Hagler, A. T.; Lifson, S. *J. Am. Chem. Soc.* **1974**, *96*, 5327. (t) Pertsin, A. J.; Nauchitel, V. V.; Kitaigorodskii, A. I. *Mol. Cryst. Liq. Cryst.* **1975**, *31*, 205. (u) Godleski, S. A.; Schleyer, P. v. R.; Osawa, E.; Inamoto, Y.; Fujikura, Y. *J. Org. Chem.* **1976**, *41*, 2596. (v) Fitzwater, S.; Bartell, L. S. *J. Am. Chem. Soc.* **1976**, *98*, 5107. (w) Bartell, L. S.; Fitzwater, S. *J. Chem. Phys.* **1977**, *67*, 4168. (x) Bartell, L. S. *J. Am. Chem. Soc.* **1977**, *99*, 3279-82. (y) Kitaigorodskii, A. I. *Chem. Soc. Rev.* **7**, 133. (z) Melberg, S.; Rasmussen, K. *J. Mol. Struct.* **1979**, *57*, 215-39. (aa) Brooks, B. R.; Bruccoleri, R. E.; Olafson, B. D.; States, D. J.; Swaminathan, S.; Karplus, M. *J. Comput. Chem.* **1983**, *4*, 187. (bb) Nilsson, L.; Karplus, M. *J. Comput. Chem.* **1986**, *7*, 591. (cc) Weiner, S. J.; Kollman, P. A.; Case, D. A.; Singh, U. C.; Ghio, C.; Alagona, G.; Profeta, S., Jr.; Weiner, P. *J. Am. Chem. Soc.* **1984**, *106*, 765. (dd) Weiner, S. J.; Kollman, P. A.; Nguyen, D. T.; Case, D. A. *J. Comput. Chem.* **1986**, *7*, 230. (ee) Allinger, N. L. *J. Am. Chem. Soc.* **1977**, *99*, 8127. (ff) Sprague, J. T.; Tai, J. C.; Yuh, Y.; Allinger, N. L. *J. Comput. Chem.* **1987**, *8*, 581.

(2) Mayo, S. L.; Olafson, B. D.; Goddard, W. A., III *J. Phys. Chem.* **1990**, *94*, 8897.

(3) Gajewski, J. J.; Gilbert, K. E.; McKelvey, J. In *Advances in Molecular Modelling*; Liotta, D., Ed.; JAI Press: Greenwich, CT, 1990; Vol. 2, p 65. Clark, M. C.; Cramer, R. D., III; Van Opdenbosch, N. *J. Comput. Chem.* **1989**, 982.

0002-7863/92/1514-10024$03.00/0

provided as supplementary material.

II. Universal Force Field

The parameters used to generate the Universal force field include a set of hybridization dependent atomic bond radii, a set of hybridization angles, van der Waals parameters, torsional and inversion barriers, and a set of effective nuclear charges.

A. Atom Types. The elements in the Universal force field periodic table are the atom types: atoms of the same type may only be similar chemically and physically, yet, as is the norm, they are treated identically in the force field. As reported here, UFF has 126 atom types. A five-character mnemonic label is used to describe the atom types. The first two characters correspond to the chemical symbol; an underscore appears in the second column if the symbol has one letter (e.g., N_ is nitrogen, Rh is rhodium). The third column describes the hybridization or geometry: 1 = linear, 2 = trigonal, R = resonant, 3 = tetrahedral, 4 = square planar, 5 = trigonal bipyramidal, 6 = octahedral. Thus N_3 is tetrahedral nitrogen, while Rh6 is octahedral rhodium. The forth and fifth columns are used as indicators of alternate parameters such as formal oxidation state: Rh6+3 indicates an octahedral rhodium formally in the +3 oxidation state, e.g., $Rh(NH_3)_6^{3+}$. H_b indicates a bridging hydrogen as in B_2H_6. O_3_z is an oxygen suited for framework oxygens of a zeolite lattice. P_3_q is a tetrahedral four-coordinate phosphorus used to describe organometallic coordinated phosphines, e.g., $(Ph_3P)_2PtCl_2$. The current UFF atom types are listed in Table I.

B. Form of the Force Field. The potential energy of an arbitrary geometry for a molecule is written as a superposition of various two-body, three-body, and four-body interactions. The potential energy is expressed as a sum of valence or bonded interactions and nonbonded interactions:

$$E = E_R + E_\theta + E_\phi + E_\omega + E_{vdw} + E_{el}$$

The valence interactions consist of bond stretching (E_R) discussed in section II.C below and angular distortions discussed in section II.D. Included as angular distortions are bond angle bending (E_θ), dihedral angle torsion (E_ϕ), and inversion terms (E_ω). The nonbonded interactions consist of van der Waals (E_{vdw}) terms discussed in section II.E and electrostatic (E_{el}) terms discussed in section II.F.

C. Bond Stretch. The universal force field describes the bond stretch interaction as either a harmonic oscillator:

$$E_R = \tfrac{1}{2}k_{IJ}(r - r_{IJ})^2 \quad (1a)$$

or as the Morse function:

$$E_R = D_{IJ}[e^{-\alpha(r-r_{IJ})} - 1]^2 \quad (1b)$$

where k_{IJ} is the force constant in units of (kcal/mol)/Å^2, r_{IJ} is the standard or natural bond length in angstroms, D_{IJ} is the bond dissociation energy (kcal/mol), and

$$\alpha = [k_{IJ}/2D_{IJ}]^{1/2} \quad (1c)$$

The Morse function is a more accurate description since it implicitly includes anharmonic terms near equilibrium (r_{IJ}) and leads to a finite energy (D_{IJ}) for breaking bonds. As with the Dreiding force field[2] for calculations using the Morse stretch, the dissociation energy (D_{IJ}) is set to $n = 70$ kcal/mol, where n is the bond order between centers I and J. The remaining parameters k_{IJ} and r_{IJ} are discussed below, and the parameterization provided below is for the harmonic form of the bond stretch.

1. Bond Radii. The natural bond length r_{IJ} is assumed to be the sum of atom type specific single bond radii, plus a bond order correction, plus an electronegativity correction:

$$r_{IJ} = r_I + r_J + r_{BO} + r_{EN} \quad (2)$$

The single bond radii r_I for H, C, N, and O were obtained by fitting a small set of organic molecules. The hydrogen radius was fit to a methyl C–H distance in propane of 1.112 Å. The carbon radii C_3, C_2, and C_1 as well as the bond order proportionality constant (discussed below) were fit to propane, propene, and propyne C–C single, single, single, double, and triple bond distances of 1.526 Å, 1.501 Å, 1.458 Å, 1.336 Å, and 1.207 Å, respectively. The radius for C_R was fit to a benzene C–C distance of 1.399 Å (bond order $1^1/_2$). The nitrogen radii N_3, N_R, N_2, and N_1 were fit to dimethylamine, *N*-methylformamide, dimethyldiazene, and acetonitrile C–N single, C–N single, N–N double, and C–N triple bond distances of 1.462 Å, 1.459 Å, 1.247 Å, and 1.157 Å, respectively. The oxygen radii O_3, O_R, and O_2 were fit to methyl ether, methyl vinyl ether, and acetone C–O single, C–O single, and C–O double bond distances of 1.410 Å, 1.428 Å, and 1.222 Å, respectively. The radius for O_1 was fit to a carbon monoxide C–O triple bond distance of 1.128 Å. The radius for O_3_z was fit to a Si–O single bond distance of 1.592 Å in $(Cl_3Si)_2O$. The radius of the bridging hydride H_b was fit to a B–H bridging bond distance of 1.320 Å in diborane.

The radii of the group 1 elements were obtained from the corresponding homonuclear gas-phase dimers.[4b] Ca, Sr, and Ba radii were taken from the X-ray structures of carboxylates,[5] using a fundamental O_3 radius of 0.657 Å. The Xe4+4 radius was obtained from square-planar XeF_4, using a fundamental F radius of 0.668 Å.[6] The Kr4+4 radius was extrapolated from KrF_2, based on the 0.07-Å decrease in Xe–F bond lengths observed in XeF_2[6] relative to XeF_4. The remaining noble gas radii were extrapolated. P_3_q was taken from the P–C bond distances of two Pt trimethylphosphine complexes, and S_2 from $[CH_3C_5H_4Mo(\mu\text{-}S)S]_2$. S_R was obtained from thiophene and Ag from pentafluorophenyl(ylide)silver(I), all using a fundamental C_R bond radius of 0.729 Å.

Radii for actinides Th6+4 through Am6+4 were extrapolated from the lanthanides, based on the 0.1-Å difference between Nd6+3 and U6+4 reference compound radii. Radii for actinides Ac6+3 and Cm6+3 through Lw6+3 were extrapolated from the lanthanides, based on the approximately 0.05-Å difference in ionic radii between lanthanide+3 and actinide+3 halides.[7]

For the remaining elements, the single bond radii were obtained directly from experimental structures of compounds containing an element–carbon single bond using a fundamental C_3 bond radius of 0.757 Å, or were interpolated. Gas-phase experimental structures were normally taken from published compilations;[8,9] X-ray structures were obtained by searching the Cambridge data base.[10] A listing of the raw bond distances, the compounds they were taken from, and the literature sources are collected in the supplementary material.

The initial observation and subsequent understanding of many important structural effects in chemistry arose by comparing "standard" bond distances (from a summation of covalent radii) with experimental bond distances. These structural-electronic effects include electronegativity, resonance, metal-ligand π bonding, metal–ligand π back-bonding, and the trans influence. A force field capable of fully predicting molecular structure must reproduce these effects. In order to account for these effects and

(4) (a) Nicholas, J. B.; Hopfinger, A. J.; Trouw, F. R.; Iton, L. E. *J. Am. Chem. Soc.* **1991**, *113*, 4792. (b) Huber, K. P.; Hertzberg, G. *Molecular Spectra and Molecular Structure. IV. Constants of Diatomic Molecules*; Van Nostrand Reinhold: New York, 1979.

(5) van der Sluis, P.; Schouten, A.; Spek, A. L. *Acta Cryst.* **1987**, *C43*, 1922. Jones, P. G. *Acta Cryst.* **1984**, *C40*, 804. Yokomori, Y.; Flaherty, K. A.; Hodgson, D. J. *Inorg. Chem.* **1988**, *27*, 2300.

(6) Levy, H. A.; Argon, P. A. *J. Am. Chem. Soc.* **1963**, *85*, 241. Templeton, D. H.; Zalkin, A.; Forrester, J. D.; Williamson, S. M. *J. Am. Chem. Soc.* **1963**, *85*, 242.

(7) Brown, D. *Halides of Lanthanides and Actinides*; Wiley-Interscience: New York, 1968.

(8) Hellwege, K.-H. *Landolt-Boernstein Numerical Data and Functional Relationships in Science and Technology*; Springer Verlag: Berlin, 1976; Vol. 7.

(9) Harmony, M. D.; Laurie, V. W.; Kuczkowski, R. L.; Schwendeman, R. H.; Ramsay, D. A.; Lovas, F. J.; Lafferty, W. J.; Maki, A. G. *J. Phys. Chem. Ref. Data* **1979**, *8*, 619.

(10) Kennard, O. Cambridge Crystallographic Data Centre, University Chemical Laboratory, Lensfield Rd., Cambridge, CBZ 1 EW, UK.

Table I. Atomic Data

atom type	valence: bond r_I[a]	valence: angle θ_0[b]	nonbond: distance x_I[a]	nonbond: energy D_I[c]	nonbond: scale ζ	effective charge Z_I*[d]
H_	0.354	180.0	2.886	0.044	12.0	0.712
H_b	0.460	83.5	2.886	0.044	12.0	0.712
He4+4	0.849	90.0	2.362	0.056	15.24	0.098
Li	1.336	180.0	2.451	0.025	12.0	1.026
Be3+2	1.074	109.47	2.745	0.085	12.0	1.565
B_3	0.838	109.47	4.083	0.180	12.052	1.755
B_2	0.828	120.0	4.083	0.180	12.052	1.755
C_3	0.757	109.47	3.851	0.105	12.73	1.912
C_R	0.729	120.0	3.851	0.105	12.73	1.912
C_2	0.732	120.0	3.851	0.105	12.73	1.912
C_1	0.706	180.0	3.851	0.105	12.73	1.912
N_3	0.700	106.7	3.660	0.069	13.407	2.544
N_R	0.699	120.0	3.660	0.069	13.407	2.544
N_2	0.685	111.2	3.660	0.069	13.407	2.544
N_1	0.656	180.0	3.660	0.069	13.407	2.544
O_3	0.658	104.51	3.500	0.060	14.085	2.300
O_3_z	0.528	146.0	3.500	0.060	14.085	2.300
O_R	0.680	110.0	3.500	0.060	14.085	2.300
O_2	0.634	120.0	3.500	0.060	14.085	2.300
O_1	0.639	180.0	3.500	0.060	14.085	2.300
F_	0.668	180.0	3.364	0.050	14.762	1.735
Ne4+4	0.920	90.0	3.243	0.042	15.440	0.194
Na	1.539	180.0	2.983	0.030	12.0	1.081
Mg3+2	1.421	109.47	3.021	0.111	12.0	1.787
Al3	1.244	109.47	4.499	0.505	11.278	1.792
Si3	1.117	109.47	4.295	0.402	12.175	2.323
P_3+3	1.101	93.8	4.147	0.305	13.072	2.863
P_3+5	1.056	109.47	4.147	0.305	13.072	2.863
P_3+q	1.056	109.47	4.147	0.305	13.072	2.863
S_3+2	1.064	92.1	4.035	0.274	13.969	2.703
S_3+4	1.049	103.20	4.035	0.274	13.969	2.703
S_3+6	1.027	109.47	4.035	0.274	13.969	2.703
S_R	1.077	92.2	4.035	0.274	13.969	2.703
S_2	0.854	120.0	4.035	0.274	13.969	2.703
Cl	1.044	180.0	3.947	0.227	14.866	2.348
Ar4+4	1.032	90.0	3.868	0.185	15.763	0.300
K_	1.953	180.0	3.812	0.035	12.0	1.165
Ca6+2	1.761	90.0	3.399	0.238	12.0	2.141
Sc3+3	1.513	109.47	3.295	0.019	12.0	2.592
Ti3+4	1.412	109.47	3.175	0.017	12.0	2.659
Ti6+4	1.412	90.0	3.175	0.017	12.0	2.659
V_3+5	1.402	109.47	3.144	0.016	12.0	2.679
Cr6+3	1.345	90.0	3.023	0.015	12.0	2.463
Mn6+2	1.382	90.0	2.961	0.013	12.0	2.43
Fe3+2	1.270	109.47	2.912	0.013	12.0	2.43
Fe6+2	1.335	90.0	2.912	0.013	12.0	2.43
Co6+3	1.241	90.0	2.872	0.014	12.0	2.43
Ni4+2	1.164	90.0	2.834	0.015	12.0	2.43
Cu3+1	1.302	109.47	3.495	0.005	12.0	1.756
Zn3+2	1.193	109.47	2.763	0.124	12.0	1.308
Ga3+3	1.260	109.47	4.383	0.415	11.0	1.821
Ge3	1.197	109.47	4.280	0.379	12.0	2.789
As3+3	1.211	92.1	4.230	0.309	13.0	2.864
Se3+2	1.190	90.6	4.205	0.291	14.0	2.764
Br	1.192	180.0	4.189	0.251	15.0	2.519
Kr4+4	1.147	90.0	4.141	0.220	16.0	0.452
Rb	2.260	180.0	4.114	0.04	12.0	1.592
Sr6+2	2.052	90.0	3.641	0.235	12.0	2.449
Y_3+3	1.698	109.47	3.345	0.072	12.0	3.257
Zr3+4	1.564	109.47	3.124	0.069	12.0	3.667
Nb3+5	1.473	109.47	3.165	0.059	12.0	3.618
Mo6+6	1.467	90.0	3.052	0.056	12.0	3.40
Mo3+6	1.484	109.47	3.052	0.056	12.0	3.40
Tc6+5	1.322	90.0	2.998	0.048	12.0	3.40
Ru6+2	1.478	90.0	2.963	0.056	12.0	3.40
Rh6+3	1.332	90.0	2.929	0.053	12.0	3.508
Pd4+2	1.338	90.0	2.899	0.048	12.0	3.21
Ag1+1	1.386	180.0	3.148	0.036	12.0	1.956
Cd3+2	1.403	109.47	2.848	0.228	12.0	1.65
In3+3	1.459	109.47	4.463	0.599	11.0	2.07
Sn3	1.398	109.47	4.392	0.567	12.0	2.961
Sb3+3	1.407	91.6	4.420	0.449	13.0	2.704
Te3+2	1.386	90.25	4.470	0.398	14.0	2.882
I_	1.382	180.0	4.50	0.339	15.0	2.65
Xe4+4	1.267	90.0	4.404	0.332	12.0	0.556
Cs	2.570	180.0	4.517	0.045	12.0	1.573
Ba6+2	2.277	90.0	3.703	0.364	12.0	2.727
La3+3	1.943	109.47	3.522	0.017	12.0	3.30
Ce6+3	1.841	90.0	3.556	0.013	12.0	3.30
Pr6+3	1.823	90.0	3.606	0.010	12.0	3.30
Nd6+3	1.816	90.0	3.575	0.010	12.0	3.30
Pm6+3	1.801	90.0	3.547	0.009	12.0	3.30
Sm6+3	1.780	90.0	3.520	0.008	12.0	3.30
Eu6+3	1.771	90.0	3.493	0.008	12.0	3.30
Gd6+3	1.735	90.0	3.368	0.009	12.0	3.30
Tb6+3	1.732	90.0	3.451	0.007	12.0	3.30
Dy6+3	1.710	90.0	3.428	0.007	12.0	3.30
Ho6+3	1.696	90.0	3.409	0.007	12.0	3.416
Er6+3	1.673	90.0	3.391	0.007	12.0	3.30
Tm6+3	1.660	90.0	3.374	0.006	12.0	3.30
Yb6+3	1.637	90.0	3.355	0.228	12.0	2.618
Lu6+3	1.671	90.0	3.640	0.041	12.0	3.271
Hf3+4	1.611	109.47	3.141	0.072	12.0	3.921
Ta3+5	1.511	109.47	3.170	0.081	12.0	4.075
W_6+6	1.392	90.0	3.069	0.067	12.0	3.70
W_3+4	1.526	109.47	3.069	0.067	12.0	3.70
W_3+6	1.380	109.47	3.069	0.067	12.0	3.70
Re6+5	1.372	90.0	2.954	0.066	12.0	3.70
Re3+7	1.314	109.47	2.954	0.066	12.0	3.70
Os6+6	1.372	90.0	3.120	0.037	12.0	3.70
Ir6+3	1.371	90.0	2.840	0.073	12.0	3.731
Pt4+2	1.364	90.0	2.754	0.080	12.0	3.382
Au4+3	1.262	90.0	3.293	0.039	12.0	2.625
Hg1+2	1.340	180.0	2.705	0.385	12.0	1.75
Tl3+3	1.518	120.0	4.347	0.680	11.0	2.068
Pb3	1.459	109.47	4.297	0.663	12.0	2.846
Bi3+3	1.512	90.0	4.370	0.518	13.0	2.470
Po3+2	1.50	90.0	4.709	0.325	14.0	2.33
At	1.545	180.0	4.750	0.284	15.0	2.24
Rn4+4	1.420	90.0	4.765	0.248	16.0	0.583
Fr	2.880	180.0	4.90	0.050	12.0	1.847
Ra6+2	2.512	90.0	3.677	0.404	12.0	2.92
Ac6+3	1.983	90.0	3.478	0.033	12.0	3.90
Th6+4	1.721	90.0	3.396	0.026	12.0	4.202
Pa6+4	1.711	90.0	3.424	0.022	12.0	3.90
U_6+4	1.684	90.0	3.395	0.022	12.0	3.90
Np6+4	1.666	90.0	3.424	0.019	12.0	3.90
Pu6+4	1.657	90.0	3.424	0.016	12.0	3.90
Am6+4	1.660	90.0	3.381	0.014	12.0	3.90
Cm6+3	1.801	90.0	3.326	0.013	12.0	3.90
Bk6+3	1.761	90.0	3.339	0.013	12.0	3.90
Cf6+3	1.750	90.0	3.313	0.013	12.0	3.90
Es6+3	1.724	90.0	3.299	0.012	12.0	3.90
Fm6+3	1.712	90.0	3.286	0.012	12.0	3.90
Md6+3	1.689	90.0	3.274	0.011	12.0	3.90
No6+3	1.679	90.0	3.248	0.011	12.0	3.90
Lw6+3	1.698	90.0	3.236	0.011	12.0	3.90

[a] Å. [b] Degrees. [c] kcal/mol. [d] Charge.

to exploit the wealth of literature data expressed in terms of covalent radii and bond orders, a Pauling-type[11] bond order correction r_{BO} is used to modify the single bond radii

$$r_{BO} = -\lambda(r_I + r_J) \ln (n) \quad (3)$$

where the proportionality constant $\lambda = 0.1332$ was determined for the set propane, propene, and propyne simultaneously with the C_3, C_2, and C_1 radii. The single bond covalent distance is included in the correction to provide the correct metric throughout the periodic table. The amide C–N bond order of 1.41 was used in order to reproduce the amide C–N bond distance of 1.366 Å in *N*-methylformamide, the C_R and N_R single bond radii having been determined above. A fractional amide bond

(11) Pauling, L. *The Nature of the Chemical Bond*; Cornell University Press: Ithaca, NY, 1960; p 239.

order is reasonable given the polar nature of the C–O π bond and the resulting parital delocalization of the nitrogen π lone pair onto carbon. Intra-ring bonds of aromatic rings are assigned bond orders based on the number of π electrons, resulting in a bond order of 1.5 for normal aromatic rings.

The electronegativity correction r_{EN} of O'Keeffe and Brese[12]

$$r_{EN} = r_I r_J(\sqrt{\chi_I} - \sqrt{\chi_J})^2/(\chi_I r_I + \chi_J r_J) \quad (4)$$

is used directly with the previously reported GMP electronegativity set.[13] For example, for a Si–O_3_z bond the electronegativity correction is 0.0533 Å.

2. Force Constants. The bond stretching force constants are atom based and are obtained from a previously reported generalization of Badger's rules.[14] Consider the following simple description of the bounding curve

$$E_R = E_0 - FR - G(Z_I^* Z_J^*/R) \quad (5)$$

where F is to be determined, Z_I^* and Z_J^* are effective charges, and $G = 332.06$ so that R is in Å, Z is in electron units, and E_R is in kcal/mol. The assumption is that the bonding is dominated by attractive ionic terms (even for H_2) plus short-range Pauli repulsions (approximated as linear). The condition for an equilibrium structure leads to

$$0 = (\partial E_r/\partial R)_0 = F - G(Z_I^* Z_J^*/R^2)$$

or

$$F = G(Z_I^* Z_J^*/r_{IJ}^2)$$

The force constant then becomes

$$k_{IJ} = \left(\frac{\partial^2 E_r}{\partial R^2}\right)_0 = 2G\frac{Z_I^* Z_J^*}{R^3} = 664.12\frac{Z_I^* Z_J^*}{r_{IJ}^3} \quad (6)$$

The Z_I^* (effective atomic charges, in electron units) are least-squares fit to a set of diatomic data representing 56 elements from Huber and Herzberg.[4b] The Z_I^* for H is set at the value for H_2, and H–C is assigned a weight of 10 in the least-squares optimization. The remaining Z_I^* (effective atomic charges) are interpolated or extrapolated. The bond radii and effective charges are listed in Table I. For reference, the UFF C–N amide force constant of 1293 kcal/mol·Å^2 can be compared to the corresponding AMBER[1dd] force constant of 980 kcal/mol·Å^2 and CHARMM[1bb] force constant of 674 kcal/mol·Å^2.

D. Angular Distortions. General Fourier expansions (see eq 7) are employed in the Universal force field to describe all angular distortions because the expansions can be constructed (1) to have derivatives that are singularity free, (2) to have the appropriate distortions for the large amplitude motions found in molecular dynamics simulations, and (3) so that the C_n coefficients can be straightforwardly chosen to satisfy appropriate, physically justified, boundary conditions.

$$E_\gamma = K\sum_{n=0}^{m} C_n \cos n\gamma \quad (7)$$

1. Angle Bend. In UFF, the angle bend term is described with a small cosine Fourier expansion in θ:

$$E_\theta = K_{IJK}\sum_{n=0}^{m} C_n \cos n\theta \quad (8)$$

where the coefficients C_n are chosen to satisfy appropriate boundary conditions including that the function have a minimum at the natural bond angle θ_0. The simple cosine Fourier expansion was chosen over the more common harmonic in θ expansion[1] because of the better description of large amplitude motions[17] as found in molecular dynamics simulations. The Fourier expansion was chosen over the mathematically equivalent (for the general nonperiodic case) harmonic in cosine θ expansion[15] owing to the straightforward and consistent extension of a Fourier expansion to symmetric/periodic coordination environments found in metallic complexes such as square planar or octahedral. Additionally, as discussed below, the Fourier expansion representation has a sound physical basis.

The simple cosine Fourier expansion was selected over the SHAPES[16] Fourier expansion form

$$E_\theta = K_{IJK}[1 + \cos(p\theta + \Psi)] \quad (9a)$$

where

$$p = \pi/(\pi - \theta_0) \quad (9b)$$

and

$$\Psi = \pi - p\theta_0 \quad (9c)$$

due to the more smoothly defined description for large θ_0 for the simple cosine Fourier expansion. As is apparent from eq 9b, as θ_0 approaches π, p, the periodicity, will increase rapidly (owing to the increasingly smaller denominator). Consider, for example, Si–O–Si linkages in zeolite structures where θ_0 is approximately 145°. If θ_0 indeed equals 145°, the function is smaller by a factor of 10 at 0° than it is at 180°, whereas if $\theta_0 = 135°$ or 150°, the function is equal valued at 0° and 180°. When $\theta_0 = 144°$, the potential is zero at $\theta_0 = 0°$. This wild oscillation is caused by p passing through the integer value, 5, at 144°.

For linear, trigonal-planar, square-planar, and octahedral coordination environments, two-term Fourier expansions are used each with a $n = 0$ term C_0 and a $n = 1$, 3, 4, or 4 term, respectively. Thus eq 8 simplifies to:

$$E_\theta = \frac{K_{IJK}}{n^2}[1 - \cos(n\theta)] \quad (10)$$

These terms are precisely the same terms as are used in the SHAPES force field for these symmetric/periodic coordination environments.

For the general nonlinear case, for example, for water, the bend function should have a minimum with $E_\theta = 0$ at $\theta = \theta_0 = 104.5°$, the second derivative at θ_0 equal to the force constant, and a maximum at 180°. For the proper choice of angular terms, consider the set of group 6 hydrides H_2O, H_2S, H_2Se, H_2Te, and H_2Po. In general, group 6 elements (O, S, Se, Te, and Po) use orthogonal unpaired p orbitals to form covalent bonds; this suggests equilibrium bond angles for the hydrides of 90° and that a cos 2θ angle term will describe angular distortion. For H_2O, however, the hydrogens are sufficiently close to each other that Pauli repulsions cause the bond angle to open up to 104.5°. This steric repulsion, with constant bond distance, is a maximum at 0° and a minimum at 180°, suggesting the addition of a cos θ angle term to the cos 2θ discussed above. This leads to a three-term Fourier expansion (for the general nonlinear case)

$$E_\theta = K_{IJK}[C_0 + C_1\cos\theta + C_2\cos 2\theta] \quad (11)$$

with the three expansion coefficients defined in:

$$C_2 = 1/(4\sin^2\theta_0) \qquad C_1 = -4C_2\cos\theta_0$$
$$C_0 = C_2(2\cos^2\theta_0 + 1) \quad (12)$$

It is interesting that, developed in this manner, the C_1 coefficient

(12) O'Keefe, M.; Brese, N. E. *J. Am. Chem. Soc.* **1991**, *113*, 3226.
(13) Rappé, A. K.; Goddard, W. A., III *J. Phys. Chem.*, submitted for publication.
(14) Badger, R. M. *J. Chem. Phys.* **1934**, *2*, 2128–131. Badger, R. M. *Ibid.* **1935**, *3*, 710–714. Pearson, R. G. *J. Am. Chem. Soc.* **1977**, *99*, 4869–4875. Ohwada, K. *J. Chem. Phys.* **1980**, *72*, 1–6. Ohwada, K. *Ibid.* **1980**, *72*, 3663–3668. Ohwada, K. *Ibid.* **1980**, *73*, 5459–5463. Ohwada, K. *Ibid.* **1981**, *75*, 1309–1312. Chang, C.-A. *J. Phys. Chem.* **1983**, *87*, 1694. Barbiric, D. A.; Castro, E. A.; Fernandez, F. M. *J. Chem. Phys.* **1984**, *80*, 289–292. Ohwada, K. *Ibid.* **1984**, *80*, 1556–1561. Halgren, T. A. *J. Am. Chem. Soc.* **1990**, *112*, 4710.
(15) Karasawa, N.; Dasgupta, S.; Goddard, W. A., III *J. Phys. Chem.* **1991**, *95*, 2260.
(16) Allured, V. S.; Kelly, C. M.; Landis, C. R. *J. Am. Chem. Soc.* **1991**, *113*, 1.

gives a measure of intrinsic 1,3 steric repulsion.

a. Standard Bond Angles. The natural angles for the group 15, 17, and 18 main group elements are obtained from standard reference structures of the parent hydrides. Thus O_3 has θ_0 = 104.5° from H_2O, while S_3 has θ_0 = 92.2° from H_2S. Exceptions include O_3_z, O_R, and N_2. The bond angles for O_3_z, O_R, and N_2 are fit to $(Cl_3Si)_2O$, methyl vinyl ether, and dimethyldiazene angles of 146°, 118.3°, and 112.3°, respectively. Where structural data are unavailable, the natural angles are extrapolated from the element above it in the periodic table. The remaining elements are all assumed to have regular octahedral, tetrahedral, trigonal, or linear structures. The natural angles are collected in Table I.

b. Force Constants. The angle bend force constants are generated using a previously reported angular generalization of Badger's rules.[14] Basically, the functional form (6) is assumed to extend to the I and K atoms of a angle bend for polyatomics, and the effective charges listed in Table I are used. Thus starting with

$$E_\theta = E_0 - F\theta - \beta(Z_I^* Z_K^*/r_{IK})$$

where F is to be determined and

$$r_{IK}^2 = r_{IJ}^2 + r_{JK}^2 - 2r_{IJ}r_{JK}\cos\theta$$

taking the second derivative of E with respect to θ yields:

$$K_{IJK} = \left(\frac{\partial^2 E}{\partial\theta^2}\right)_0 = \beta\frac{Z_I^* Z_K^*}{r_{IK}^5} r_{IJ}r_{JK}[^3r_{IJ}r_{JK}(1 - \cos^2\theta_0) - r_{IK}^2\cos\theta_0] \quad (13)$$

where the distances r_{IJ} and r_{JK} are as defined in (2) above and β is an undetermined parameter. From an examination of the bending vibrational frequences of AX_4, A = C, S, Ge, and Sn and X = H, F, Cl, Br, and I, it was determined that

$$\beta = 664.12/r_{IJ}r_{JK}$$

leads to the best compromise functional form. For reference, the UFF C–N–C amide force constant of 105.5 kcal/mol·rad^2 can be compared to the corresponding AMBER[1dd] force constant of 100 kcal/mol·rad^2 and CHARMM[1bb] force constant of 70 kcal/mol·rad^2.

2. Torsion. The torsional terms for two bonds IJ and KL connected via a common bond JK is described with a small cosine Fourier expansion in ϕ:

$$E_\phi = K_{IJKL}\sum_{n=0}^{m} C_n\cos n\phi_{IJKL} \quad (14)$$

where K_{IJKL} and the coefficients C_n are determined by the rotational barrier V_ϕ, the periodicity of the potential, and the equilibrium angle. For a given central J–K bond, all torsions about this bond are considered, with each torsional barrier being divided by the number of torsions present about this J–K bond. The present torsional periodicities and minima are the same as those described in the recently published DREIDING force field[2] with modifications to the torsional barriers V_ϕ to account for periodic trends. Using the present Fourier representation (eq 14) for the torsional potential, $C_0 = 1$, $C_n = -\cos n\phi_0$, and $K_{IJKL} = {}^1/_2V_\phi$ which yields

$$E_\phi = {}^1/_2V_\phi[1 - \cos n\phi_0\cos n\phi] \quad (15)$$

Specific general cases include (a) j = an sp^3 center and k = an sp^3 center where n = 3 and ϕ_0 = 180° (or 60°), (b) j = an sp^2 center and k = an sp^3 center where n = 6 and ϕ_0 = 0° (V_ϕ = 1 kcal/mol), and (c) j = an sp^2 center and k = an sp^2 center of variable bond order where n = 2 and ϕ_0 = 180° (or 60°).

The torsional barriers involving a pair of sp^3 centers (V_{sp^3}) are fit to experimental data for the parent hydride compounds (see Table II) with the torsional barriers obtained from:

$$V_{sp^3} = \sqrt{V_jV_k} \quad (16)$$

Table II. Torsional Barriers (kcal/mol)

bond	experimental	calculated
CH_3–CH_3	2.93[a]	2.90
CH_3–SiH_3	1.7[a]	1.7
CH_3–GeH_3	1.2[a]	1.2
CH_3–SnH_3	0.65[a]	0.65
CH_3–NH_2	2.0[a]	2.0
CH_3–PH_2	2.0[a]	2.0
CH_3–AsH_2	1.5[a]	1.5
CH_3–OH	1.1[a]	1.0
CH_3–SH	1.3[a]	1.3
CH_3–SeH	1.0[a]	1.0
trans HO–OH	1.1[a]	1.7
cis HO–OH	7.0[a]	6.6
trans HS–SH	6.8[a]	6.8
cis HS–SH	7.2[a]	7.2
anisole	4.6[b]	3.6
thioanisole	1.0[b]	1.7
acetaldehyde	1.17[a]	0.83
isoprene	2.71[c]	1.56
ethylbenzene	1.16[c]	3.16

[a] Lister, D. G.; Macdonald, J. N.; Owen, N. L. *Internal Rotation and Inversion*; Academic Press: New York, 1978; pp 164, 165. [b] Schaefer, T.; Penner, G. H. *Can. J. Chem.* **1988**, *66*, 1641. [c] Compton, D. A. C.; George, W. O.; Maddams, W. F. *J. Chem. Soc., Perkin Trans. 2* **1976**, 1666. [d] Miller, A.; Scott, D. W. *J. Chem. Phys.* **1978**, *68*, 1317.

Table III. sp^3 Torsional Barrier Parameters

atom type	V_j (kcal/mol)	atom type	V_j (kcal/mol)	atom type	V_j (kcal/mol)
C_3	2.119	S_3	0.484	Sb3	1.1
N_3	0.450	Ge3	0.701	Te3	0.3
O_3	0.018	As3	1.5	Pb3	0.1
Si3	1.225	Se3	0.335	Bi3	1.0
P_3	2.400	Sn3	0.199	Po3	0.3

The V_j values are collected in Table III.

Torsional barriers involving a pair of sp^2 centers (V_{sp^2}) with variable bond order are assigned barriers using eq 17 where BO_{jk} is the bond order between atoms j and k.

$$V_{sp^2} = 5\sqrt{U_jU_k}(1 + 4.18\ln(BO_{jk})) \quad (17)$$

The constants 5 and 4.18 were obtained from fitting the low energy a_u, b_{1u}, and b_{2g} vibrational modes of ethylene,[18] the gas-phase barrier of *N,N*-dimethylformamide ($\Delta H^\ddagger$ = 19.7 kcal/mol),[19] and the low-energy e_{2u}, a_{2u}, and b_{2g} vibrational modes of benzene.[18] The U_j constants are assigned values of 2, 1.25, 0.7, 0.2, and 0.1 for the first through sixth periods (based roughly on the group 4 V_j values discussed above), respectively.

As in the DREIDING force field,[2] the torsional terms for sp^3 group 6 central atoms are treated as exceptions based on valence considerations which suggest that the bonds have a dihedral angle of 90°. For a single bond involving a pair of group 6 sp^3 atoms, eq 16 is used with V_J = 2 kcal/mol for oxygen and V_J = 6.8 kcal/mol for the remaining group 6 elements (fit for H_2O_2 and H_2S_2[20]). For this case the periodicity (n) is 2 and the equilibrium angle ϕ_0 is 90°. For a single bond involving a sp^3 atom of the oxygen column and an sp^2 or resonant atom of another column, eq 17 is used directly. For this case the periodicity (n) is 2 and the equilibrium angle ϕ_0 is 90°. The torsional potentials for central bonds involving non-main-group elements were assigned a value of zero. Torsional potentials for central bonds involving sp-hy-

(17) The inadequacy of a harmonic in θ representation has been reported previously; see, for example, Figure 1 of ref 16 and Figure 3 of ref 4a. An additional discussion of problems with angular potentials is provided in: Swope, W. C.; Ferguson, D. M. *J. Comput. Chem.* **1992**, *13*, 585.

(18) Shimanouchi, T. *Tables of Molecular Vibrational Frequencies*; NSRDS-NBS 39; U.S. Government Printing Office: Washington, DC.; 1972.

(19) Ross, B. D.; True, N. S. *J. Am. Chem. Soc.* **1984**, *106*, 2451.

(20) Lister, D. G.; Macdonald, J. N.; Owen, N. L. *Internal Rotation and Inversion*; Academic Press: New York, 1978; pp 164–165.

bridized centers X_1 were assigned a value of zero. In addition, when angles about the central atoms approach 180°, the potential energy and derivative terms are set to zero as is conventionally done.

The remaining exception is for the case of a single bond involving one sp^2 atom and one sp^3 atom where the sp^2 atom is bonded to another sp^2 atom (e.g., propene). For this case we use $V_0 = 2.0$ kcal/mol, $n = 3$, and $\phi_0 = 180°$.

The overall reproduction of torsional barriers is quite good (see Table II). The C_3-sp^3 barriers were chosen to fit the experimental barriers, the H_2O_2 and H_2S_2 values were best compromise values, and anisole, thioanisole, acetaldehyde, isoprene, and ethylbenzene are tests of eq 17.

3. Inversion. For UFF, a one- or two-term cosine Fourier expansion in ω is used for atoms I bonded exactly to three other atoms J, K, L:

$$E_\omega = K_{IJKL}(C_0 + C_1 \cos \omega_{IJKL} + C_2 \cos 2\omega_{IJKL}) \quad (18)$$

where K_{IJKL} is the force constant in (kcal/mol) and ω_{IJKL} is the angle between the IL axis and the IJK plane. For a given central atom I there are three unique axes (IL, IJ, and IK); all three are considered, with each inversion barrier being divided by the number of inversions present (three) about center I. The cos 2ω term yields a minimum for $\omega = 90°$ and a maximum for $\omega = 0°$ as would be appropriate for PH_3. The cos ω term yields a minimum for $\omega = 0°$ and a maximum for $\omega = 180°$ as would be appropriate for ethylene. Linear combinations of these terms will describe all intermediate cases. The inversion potential can also be expressed in terms of the computationally convenient normal to the IJK plane and the angle that the IL axis makes with respect to the normal to the IJK plane, γ_{IJKL}. The two forms are related by $\omega = \gamma - \pi$.

$$E_\gamma = K_{IJKL}(C_0 + C_1 \sin \gamma_{IJKL} + C'_2 \cos 2\gamma_{IJKL}) \quad (19)$$

For C_2 and C_R sp^2 atom types with exactly three substituents, $C_0 = 1$, $C_1 = -1$, and $C_2 = 0$. If carbon is bonded to O_2, the force constant is set to 50 kcal/mol, as fit to the b_2 wag of formaldehyde; otherwise, the force constant is set to 6 kcal/mol, as fit to the low-energy a_u, b_{1u}, and b_{2g} vibrational modes of ethylene and the low-energy e_{2u}, a_{2u}, and b_{2g} vibrational modes of benzene.[18] Force constants for groups 5 and 6 were chosen to fit the experimentally observed inversion barriers for the group 5 hydrides NH_3 and PH_3.[21] The ω_0 were obtained from standard reference structures of the hydrides and the C_n coefficients fit to a minimum with $E_\omega = 0$ at $\omega = \omega_0$ and that E_ω for the maximum at $\omega = 0°$ be equal to $E_{barrier}$. In order to fit observed barriers, inversion terms corresponding to $E_{barrier} = 0$ for nitrogen and 22 kcal/mol for P, As, Sb, and Bi are used. The inversion force constants for all other atom types are set to zero.

E. van der Waals. Nonbonded interactions (van der Waals forces) are included in the Universal force field. A Lennard-Jones 6–12 type expression is used:

$$E_{vdw} = D_{IJ}\left\{-2\left[\frac{x_{IJ}}{x}\right]^6 + \left[\frac{x_{IJ}}{x}\right]^{12}\right\} \quad (20)$$

where D_{IJ} is the well depth in kcal/mol and x_{IJ} is the van der Waals bond length in Å. The 6–12 Lennard-Jones form is chosen over an exponential-6 form (discussed below) for its numerical stability; the exponential-6 form blows up for small internuclear separations. A complete set of exponential-6 parameters are provided in Table I although the valence parameterization discussed above actually used Lennard-Jones 6–12 nonbond potentials.

As is conventionally done, the general x_{IJ} and D_{IJ} are obtained from the homonuclear parameters through the use of combination rules. The choice of combination rules for the Lennard-Jones distances is somewhat problematic. The use of an arithmetic mean for the Lennard-Jones distance,

$$x_{IJ} = \tfrac{1}{2}(x_I + x_J) \quad (21a)$$

where x_I is the atomic van der Waals distance, is analogous to the summing of covalent radii as used in eq 2 above for bond distances. Use of a geometric mean combination rule for distance

$$x_{IJ} = \sqrt{x_I \times x_J} \quad (21b)$$

facilitates summation of van der Waals terms for crystalline systems. The molecular parameters (distances, angles, inversion barriers, and torsional barriers) are developed here using geometric distance combination rules. UFF assumes standard geometric combination rules for the well depth:

$$D_{IJ} = (D_I D_J)^{1/2} \quad (22)$$

where D_I is the atomic van der Waals energy. Values of the van der Waals distances x_I and D_I for UFF are listed in Table I.

The most difficult part of developing a general force field is the assignment of van der Waals parameters. The present Lennard-Jones van der Waals parameters are developed within the conceptual framework of the exponential-6 form. This functional form is physically based on the short-range exponential repulsion arising from Pauli orthogonalization and the long-range $1/r^6$ induced dipole-induced dipole dispersive attraction:

$$E_{vdw} = Ae^{-Bx} - C_6/x^6 \quad (23)$$

The repulsive exponential B and the dispersive attractive term C_6 are developed below for the entire periodic table. The third degree of freedom contained in eq 23 is determined from an empirical relation obtained between literature values of Lennard-Jones distances and the present repulsive exponentials B.

The repulsion exponent B can be developed from a consideration of the physical basis of the repulsive term, that is, the repulsive interaction between pairs of closed shells. This repulsive interaction to first order is proportional to the overlap between the wave functions squared. We begin with the approximate relation[22] that the long-range distance dependence of a wave function is

$$\Psi \sim e^{-(\sqrt{2IP})r} \quad (24)$$

The overlap between a pair of exponential functions (with the same Slater exponent ξ) is

$$S = (1 + \xi r + \tfrac{1}{3}(\xi r)^2)e^{-\xi r} \quad (25)$$

Thus the repulsive interaction (S^2) between a pair of atoms

$$S^2 \sim e^{-2\xi r} \quad (26)$$

is directly related to the electron density where, from eq 24

$$\xi = \sqrt{2IP} \quad (27)$$

This leads to the exponent in the exponential-6 being defined as

$$B = 2\xi = 2\sqrt{2IP} \quad (28)$$

The ionization energy for each atom I (IP_I) in the entire periodic table can be obtained from the sum of the GMP electronegativity and idempotential:[13]

$$IP_I = \chi_I + \tfrac{1}{2}J_I \quad (29)$$

The dispersion terms C_6 are taken as proportional to the upper bound numerical Hartree–Fock values presented by Fraga, Karwowski, and Saxena (FKS).[23]

$$C_6 = C_6^{FKS}/S \quad (30)$$

A plot of the FKS values for the noble gases versus the semiempirical values reported by Kumar and Meath[24] is used to obtain

(21) Lister, D. G.; Macdonald, J. N.; Owen, N. L. *Internal Rotation and Inversion*; Academic Press: New York, 1978; pp 179–180.

(22) Handy, N. C.; Marron, M. T.; Silverston, H. J. *Phys. Rev.* **1969**, *180*, 45.

(23) Fraga, S.; Karwowski, J.; Saxena, K. M. S. *Handbook of Atomic Data*; Elsevier Scientific: Amsterdam, 1976.

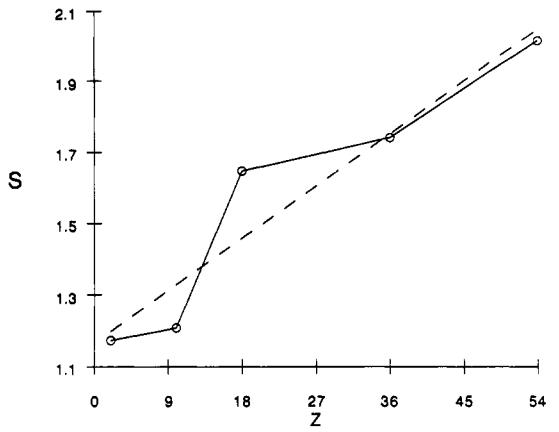

Figure 1. A plot of the Kraga, Karwowski, and Saxena C_6 dispersion terms versus the semiempirical values of Kumar and Meath. The line is the least-squares fit.

the Z-dependent scaling equation, eq 31 (see Figure 1) (R = 0.948).

$$S = 1.166 + 0.01626Z \tag{31}$$

That there should be a linear relationship between the correlation error in a Hartree–Fock calculation and the number of electrons (Z) is quite reasonable. The use of scaled C_6 terms has previously been reported, though a different scaling scheme was used.[25]

The third degree of freedom in eq 23 can be obtained by rearranging eq 23 into a mathematically equivalent form[2] containing a well depth term D_{IJ}, a distance term x_{IJ}, and a shape parameter ζ:

$$E_{vdw} = \left[D_{IJ}\left(\frac{6}{\zeta-6}\right)e^{\zeta}\right]e^{-\zeta(x/x_{IJ})} - \left[D_{IJ}\left(\frac{\zeta}{\zeta-6}\right)x_{IJ}{}^6\right]\Big/ x^6 \tag{32}$$

A comparison of like terms in eq 23 and 32 leads to eq 33 for the distance,

$$x_I = \zeta/B_I \tag{33}$$

eq 34 for the well depth

$$D_I = C_{6II}\left(\frac{\zeta-6}{\zeta}\right)\Big/ x_I{}^6 \tag{34}$$

and eq 35 for the repulsive preexponential term.

$$A_I = D_I\left(\frac{6}{\zeta-6}\right)e^{\zeta} \tag{35}$$

As discussed previously,[2] there are three simple choices for this third parameter ζ: (1) assign a value of 12 to ζ, which results in the Lennard-Jones and exponential-6 forms having precisely the same long-range distance dependence; (2) assign a value of 13.772 to ζ, which gives the exponential-6 and 6–12 forms the same curvature at the bottom of the well; or (3) fit ζ to a discrete set of crystal structures for each element. Figure 2 shows the Lennard-Jones curves for three values of ζ with B and C_6 fixed. Given the extreme sensitivity of the resulting Lennard-Jones parameters to the choice of ζ, the enormity of the challenge of fitting parameters for the entire periodic table, and the difficulty in factoring out special intermolecular bonding interactions in the crystal structures of the elements,[26,27] we have chosen to use the available data and empirically estimate ζ as discussed below.

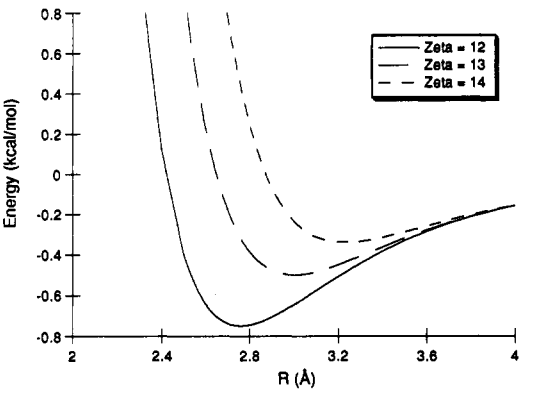

Figure 2. Plot of an exponential-6 van der Waals term as a function of ζ = 12, 13, and 14 with B_I set to 4.3333 Å^{-1} and C_{6I} set to 676.929 (kcal/mol)/Å^6.

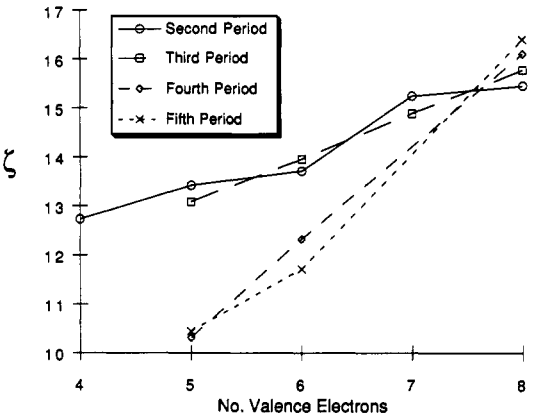

Figure 3. Plots of ζ (shape parameter) versus number of valence electrons for the second through fifth periods.

Table IV. van der Waals Parameters

		literature		Universal	
element	ref	X_I	D_I	X_I	D_I
C	15	3.898	0.095	3.851	0.105
N	27	3.662	0.077	3.660	0.069
O	27	3.405	0.096	3.500	0.060
F	27	3.472	0.073	3.364	0.050
Ne	*a*	3.243	0.072	3.243	0.042
P	2	4.15	0.32	4.147	0.305
S	2	4.03	0.344	4.035	0.274
Cl	2	3.950	0.283	3.947	0.227
Ar	*a*	3.867	0.239	3.868	0.185
As	*a*	3.35	0.6	4.230	0.309
Se	*b*	3.70	0.517	4.205	0.291
Kr	*a*	4.165	0.329	4.141	0.220
Sb	*a*	3.54	0.5	4.420	0.449
Te	*b*	3.74	1.23	4.470	0.398
Xe	*a*	4.512	0.457	4.404	0.332

[a] Fit to the elemental crystal structure, this work. [b] Fit to the elemental crystal structure, WAG unpublished results.

Using the B_I defined by eqs 28 and 29 and literature values[2,28] for exponential-6 or 6–12 x_I's, linear relations are observed for ζ (which is B_I/x_I) as a function of the number of valence electrons and row in the periodic table (see Figure 3). The scatter in the plot for the second period can be attributed largely to the choice of partial charges for the molecules used in the determination of the x_I parameters from X-ray crystal structures. Given the uncertainty in partial charge assignment, we have chosen to use two neutral cases ζ = 12.73 for C, from graphite[15] and ζ = 15.44 for

(24) Kumar, A.; Meath, W. J. *Mol. Phys.* **1985**, *54*, 823.
(25) Spackman, M. A. *J. Chem. Phys.* **1986**, *85*, 6579.
(26) Hsu, L. Y.; Williams, D. E. *Acta Cryst.* **1985**, *A41*, 296.
(27) Desiraju, G. R.; Parthasarathy, R. *J. Am. Chem. Soc.* **1989**, *111*, 8725.
(28) Williams, D. E. *Acta Cryst.* **1974**, *A30*, 71. Williams, D. E.; Starr, T. L. *Comput. Chem.* **1977**, *1*, 173. Williams, D. E.; Hsu, L. Y. *Acta Cryst.* **1980**, *A36*, 277. Cox, S. R.; Hsu, L. Y.; Williams, D. E. *Ibid.* **1981**, *A37*, 293. Williams, D. E.; Cox, S. R. *Ibid.* **1984**, *B40*, 404. Williams, D. E.; Houpt, D. J. *Ibid.* **1986**, *B42*, 286.

Ne to obtain a linear relation, eq 36, for the second period.

$$\zeta = 10.02 + 0.6775n \quad (36)$$

For the third period a least-squares fit to the x_I data in Table IV (for the third period) leads to:

$$\zeta = 8.587 + 0.897n \quad (37)$$

The discontinuity in slope between the third and fourth periods in Figure 3 can be attributed to the onset of special intermolecular bonding interactions in the solids;[26,27] P and S are both nonmetals but As and Se are both metallic or near metallic. These special bonding interactions should not be included in a van der Waals parameter set. Thus, for the remaining main group elements, eq 38 is used wherein a slope of 1 is assumed (extrapolated from the slopes of eq 36 and 37 and the noble gases are assigned a value of 15.

$$\zeta = 8 + n \quad (38)$$

The repulsive exponentials B and dispersion terms C_6 along with the shape parameters ζ are used to define the Lennard-Jones distances x_I and well depths using eq 33 and 34.

The thus obtained Lennard-Jones parameters provide reasonable estimates for the elements in their atomic state. A comparison of the UFF Lennard-Jones parameters with literature values for several elements is provided in Table IV.

For metals in positive oxidation states, the above estimates are not appropriate. For cationic metals we have obtained ionic C_{6I^+} and B_{I^+} as follows. The exponent B_{I^+} is defined as

$$B_{I^+} = 2\sqrt{2IP2_I} \quad (39)$$

where $IP2_I$ is the second ionization energy for atom I as obtained from the GMP electronegativity and idempotential[13]

$$IP2_I = \chi_I + {}^3/_2 J_I \quad (40)$$

The C_{6I^+} are obtained by scaling the neutral C_{6I} terms by the ratio of the London estimates for the neutral and positive ion C_6's

$$C_6 \sim IP\alpha^2 \quad (41)$$

thus,

$$C_{6I^+} = C_{6I}(IP_I\alpha_I^2/IP^+{}_I\alpha^+{}_I^2) \quad (42)$$

where $IP^+{}_I$ and IP_I are the experimental first and second ionization energies of atom I, and α_I and $\alpha^+{}_I$ are the FKS polarizabilities for the metallic neutral and positive ions. Setting ζ to 12 for the metallic ions the Lennard-Jones distance, x_{I^+} can be directly obtained from eq 33 and D_{I^+} from eq 34.

These Lennard-Jones parameters provide reasonable values for elements in a cationic state. For example, the UFF distance and well depth of $x_I = 3.148$ Å and $D_I = 0.036$ kcal/mol for Ag can be compared with a distance parameter of $x_I = 3.100$ Å obtained by fitting the crystal structure for AgCl with a *QEq* partial charge on Ag of 0.62 and a D_I assigned a value of 0.036 kcal/mol. The experimental cell parameter for AgCl is 5.556 Å;[29] if the UFF Ag^+ parameters are used, a cell constant of 5.592 Å is obtained. For metals with one electron in the valence shell, the above procedure breaks down; the discontinuity in the IP versus charge curve associated with removing an electron from the core, rather than an additional valence electron, is likely responsible. For the group 1 elements we have chosen to fit the distance parameters to experimental lattice parameters with assumed well depths. The results of the fits are provided in Table V.

The derived van der Waals parameters can be compared to van der Waals parameters in the literature explicitly fit to crystal properties. The present hydrogen radius and well depth of 2.886 Å and 0.044 kcal/mol are nearly the same as the Lennard-Jones radius and well depth of 2.9267 Å and 0.0335 kcal/mol fit to polyethylene.[15] The present carbon radius and well depth of 3.851 Å and 0.105 kcal/mol are nearly the same as the Lennard-Jones radius and well depth of 3.805 Å and 0.069 kcal/mol fit to graphite.[15]

Table V. Optimized Alkali Lennard-Jones Parameters

metal	a_{exp}[a]	a_{calc}[a]	D_{II}[b]	X_{II}[a]
LiF	4.026	4.026	0.05	2.298
NaF	4.628	4.629	0.06	2.824
KF	5.344	5.344	0.07	3.637
RbF	5.64	5.64	0.08	3.937
CsF	6.002	6.002	0.09	4.335

[a] Angstroms. [b] In kcal/mol.

F. Electrostatic Interactions. The valence parameters discussed in the above sections were obtained without partial charges. When included, electrostatic interactions are calculated by:

$$E_{el} = 332.0637(Q_iQ_j/\epsilon R_{ij}) \quad (43)$$

Q_i and Q_j are charges in electron units, R_{ij} is the distance in angstroms, and ϵ is the dielectric constant. The default dielectric constant is 1 for UFF and no distance cutoff is used. Partial charges are obtained using the recently published *QEq* charge equilibration scheme.[30]

G. Nonbonded Exclusions. With UFF we follow the usual convention of excluding van der Waals and electrostatic interactions for atoms that are bonded to each other (1,2 interactions) or bonded to a common atom (1,3 interactions).

III. Calculational Results and Summary

Detailed comparisons of conformational energetics and molecular structures with experimental and published MM2(3) results for organic compounds[31] and application of UFF to predict structures of main group,[32] transition metal inorganic, and organometallic compounds[33] are the subjects of future papers. Here we present the results on a select set of molecules to demonstrate the overall utility of the approach. We begin with structural comparison for a few organic molecules where the bond order varies to demonstrate the utility of a radius plus bond order correction distance function, eq 2. This is followed by three main group inorganic molecules: octamethylcyclotetrasiloxane, 1,3,5,7-tetrakis(trifluoromethyl)-2,4,6,8,9,10-hexathia-1,3,5,7-tetragermaadamantane, and dodecaphenylcyclohexastannane. We conclude with calculations on a set of transition metal complexes including tris(hexamethyldisilylamide)scandium(III), (L- or D-alanine-*N*-acetato)(L-histidinato)chromium(III), bis(*N*-allylsalicylidineiminato)nickel(II), and 1,2-bis(dimethylphosphino)ethane(neopentylidyne)(neopentylidene)(neopentyl)tungsten(VI).

A. Procedure. Minimizations were carried out on a IRIS 4D20 using a Newton–Raphson minimization scheme with a norm of the gradient convergence criteria of 1×10^{-10} (kcal/mol)/Å and were verified as minima by the absence of negative eigenvalues in the force constant matrix. Saddle points for torsional barriers were obtained using a hill climbing algorithm and were verified by the presence of a single negative eigenvalue in the force constant matrix.

B. Organics. The C_3, C_2, and C_1 radii as well as λ of eq 3 were chosen to reproduce the various C–C distances of propane, propene, and propyne. From the results presented in Figure 4 (experimental quantities in parentheses), it is apparent that it is possible to reproduce the five unique distances in the set with four adjustable parameters (three radii plus bond order scaling parameter λ). Further, the experimental C–H distances in propene and propyne are also reproduced. The angles are less well reproduced: the C–C–C angles of propane and propene are underestimated by 1.1° and 2.3°. Further, the central C–C bond of butadiene is long by 0.006 Å, and the C–C double bonds of

(29) *Crystal Data Determinative Tables*; Ondik, H. M., Wolten, G. M., Eds.; U.S. Department of Commerce: Washington, DC, 1973; Vol. II.

(30) Rappé, A. K.; Goddard, W. A., III *J. Phys. Chem.* **1991**, *95*, 3358.

(31) Casewit, C. J.; Colwell, K. S.; Rappé, A. K. *J. Am. Chem. Soc.*, second of three papers in this issue.

(32) Casewit, C. J.; Colwell, K. S.; Rappé, A. K. *J. Am. Chem. Soc.*, third of three papers in this issue.

(33) Rappé, A. K.; Colwell, K. S.; Casewit, C. J. Manuscript in preparation.

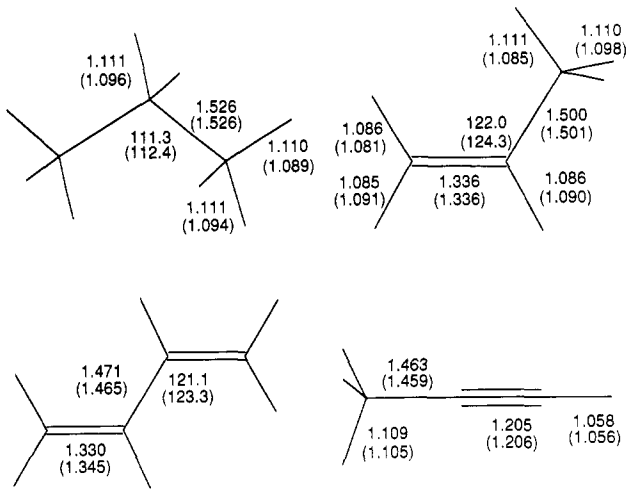

Figure 4. Sample hydrocarbon structures; experimental structural parameters in parentheses.

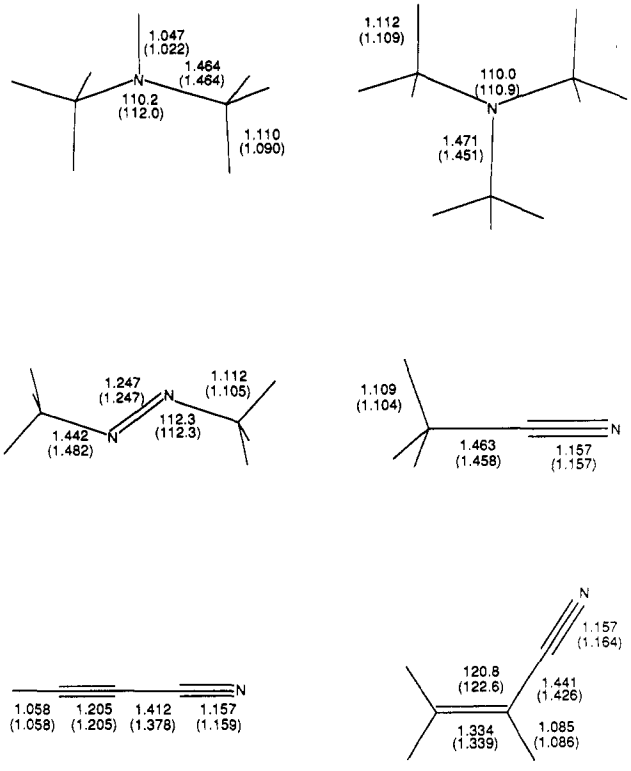

Figure 5. Sample nictinohydrocarbon structures; experimental structural parameters in parentheses.

butadiene are calculated to be 0.015 Å short. This pattern for butadiene indicates that partial (but not substantial) π bonding between the central carbons is not being accounted for in the force field.

For nitrogen-containing organic molecules, the experimental structures are reasonably well described except for cases with partial π bonding which is not included in this version of UFF. For dimethylamine (see Figure 5), the N–H distance is 0.025 Å too long and the C–N–C angle 1.8° too small, though the angle has opened up significantly (110.2°) from the equilibrium angle of N_3 (106.7°). For trimethylamine the C–N–C angle is only 0.9° too small, though the C–N distances are 0.02 Å large. The C–N distance is underestimated by 0.04 Å in dimethyldiazene, but the remaining geometric parameters are well reproduced. For acetonitrile, the C–C single bond distance is 0.005 Å long. For 2-cyano-1-ethylene the calculated C–C single bond is overestimated by 0.034 Å, indicating partial π bonding between the centers. For 2-cyano-1-ethylene the C–C double bond is 0.005

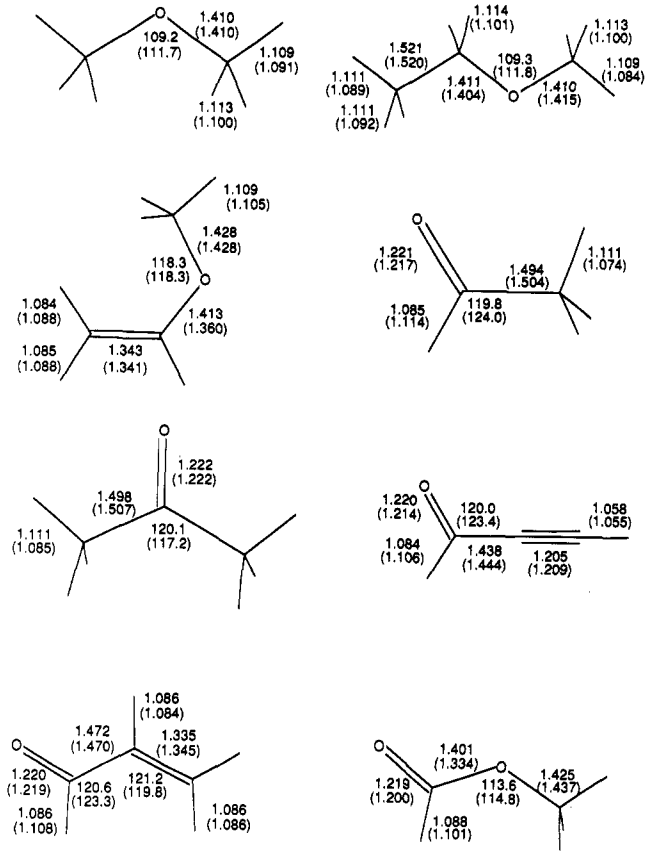

Figure 6. Sample oxohydrocarbon structures; experimental structural parameters in parentheses.

Å short, the C–N triple bond is 0.007 Å short, and the C–C single bond is 0.015 Å long also indicative of partial π bonding not accounted for in the force field.

Reasonable agreement with experiment is also found for oxygen-containing organic molecules (see Figure 6). The C–O–C angle of dimethyl ether is 2.5° smaller than experiment, though it does open up (109.2°) significantly from the equilibrium angle of 104.51°. For methyl ethyl ether the calculated C–C distance is 0.001 Å long; the *O*-methyl and *O*-ethyl distances are 0.005 Å too short and 0.007 Å too long, respectively. The C–O–C angle is 2.5° too small. For methyl vinyl ether the computed C–C double bond is 0.002 Å long, the C–O single bond is fit exactly, but the vinyl C–O distance is 0.053 Å long, indicative of partial π bonding being ignored. The C–O double bond of acetaldehyde is overestimated by 0.004 Å, and the C–C bond is underestimated by 0.01 Å. For acetone the C–C single bonds are 0.009 Å short and the C–C–C angle is 2.9° large. For propynal the C–O double bond is 0.006 Å long, the C–C single bond is well reproduced, and the C–C triple bond is 0.004 Å short. The calculated C–O double bond of acrolein is 0.001 Å long, the C–C single bond is 0.002 Å long, and the C–C double bond is 0.01 Å short. For methyl formate the C–O double bond is 0.019 Å long, the ester C–O single bond is 0.067 Å long (indicative of missing π delocalization), and the other C–O single bond distance is 0.012 Å short.

For amides the calculated structures are acceptable (see Figure 7). The calculated C–O double bond of acetamide is 0.002 Å too long, the C–C single bond is 0.021 Å too short, and the C–N resonating bond is 0.015 Å too short. For *N*-methylformamide the calculated C–O double bond is 0.001 Å short, the C–N resonating bond is 0.001 Å short, and the C–N single bond is fit. The C–N–C angle is 0.7° larger than experiment.

For organic molecules with bonds without partial π bonding, the force field reproduces the experimental organic structures to within 0.02 Å and 2°.

C. Main Group. For molecules with main group–main group bonds, experimental structures are reasonably well described in

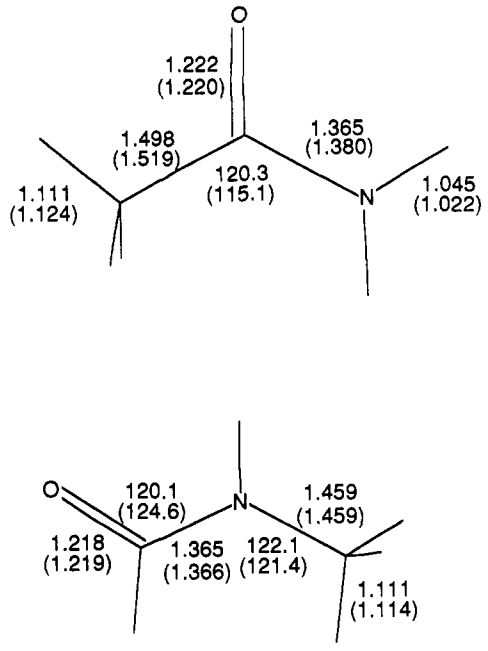

Figure 7. Sample amide structures; experimental structural parameters in parentheses.

this version of UFF. Sample molecular structures are collected in Figure 8 and the individual molecules discussed below.

Octamethylcyclotetrasiloxane.[34] X-ray studies have shown that this eight-membered siloxane ring is puckered, with Si–O–Si angles of 142°. As discussed in the main group benchmark paper,[32] the correct description of Si–O–Si linkages by molecular mechanics is still a matter of concern; the Si–O bond distances and Si–O–Si angles are very sensitive to the nature of the other substituents bound to Si. Agreement between UFF and experiment is fair for this molecule. The calculated Si–O distances are 0.058 Å short and the Si–O–Si bond angle is 3.1° large. The calculated Si–C distances are 0.054 Å short and the C–Si–C angles are 3.6° large. The O–Si–O bond angle is only 0.5° too large.

1,3,5,7-Tetrakis(trifluoromethyl)-2,4,6,8,9,10-hexathia-1,3,5,7-tetragermaadamantane.[35] The three-dimensional structure of this Ge–S analogue of adamantane is well reproduced by UFF. The calculated Ge–S bond distances are only 0.011 Å long. The Ge–C distances are 0.05 Å short and the F–C distances are 0.07 Å long. The calculated S–Ge–S angles are only 0.9° large and the Ge–S–Ge angles are 2.4° small.

Dodecaphenylcyclohexastannane.[36] In contrast to the difficulties encountered in correctly predicting Si–Si bond lengths as reported in the organic benchmark paper,[31] the structure of this Sn ring is well reproduced by UFF. The calculated Sn–Sn bond distances are underestimated by only 0.001 Å, and the Sn–C distances are underestimated by 0.036 Å. The calculated Sn–Sn–Sn angles are 1.8° small and the C–Sn–C angles are 3.6° large. The Sn–Sn–Sn–Sn dihedral angle is 5.3° large.

D. Organotransition Metal Compounds. For molecules containing metallic elements, experimental structures are reasonably well described in this version of UFF. Sample molecular structures are collected in Figure 9 and the individual molecules discussed below.

Tris(hexamethyldisilylamide)scandium(III).[37] X-ray studies have shown that the molecule is pyramidal with planar tris(silylamide) groups. The calculated N–Sc–N bond angles are only 0.7° smaller than experiment. The calculated silicon–carbon bonds are overestimated by 0.01 Å to 0.02 Å. As discussed in the metal

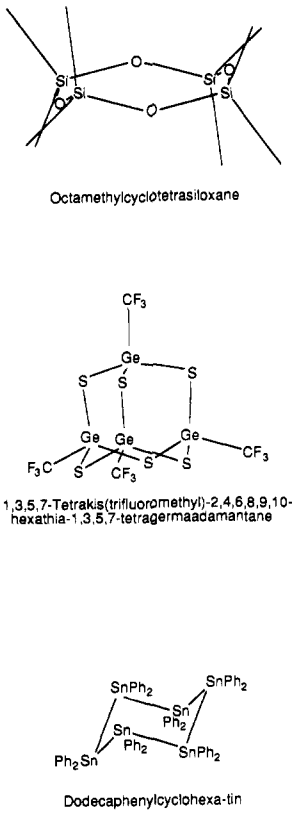

Figure 8. Structural formulas and numbering of atoms for a set of main group molecules.

benchmark paper,[33] the Sc–N amide bond distances are well described if a bond order of $^3/_2$ is used; the bonds are only short by 0.014 Å on average.

(L- or D-Alanine-*N*-acetato)(L-histidinato)chromium(III).[38] X-ray analysis of this classical coordination complex shows the environment around Cr is a distorted octahedral. UFF can only partially reproduce the distortion, with bond angle errors of up to 8°. The H-bonding network observed in the experimental structure likely contributes to the distortion from octahedral symmetry. This H-bonding effect is not included in the force field. Fair agreement between UFF and experiment is observed for the Cr–ligand distances: the calculated Cr–O bond distances, on average, are 0.047 Å short; the histidine Cr–N distance is 0.117 Å long using a bond order $^1/_2$ (the distance would be 0.047 Å short using a bond order of 1); and the calculated amino Cr–N distances are 0.078 Å and 0.058 Å long.

***cis*-Bis(2,7-dimethyl-3,6-diaza-3,5-octadiene)dichlororuthenium(II).**[39] With the exception of the Ru–N distances the coordination environment calculated by UFF is in good agreement with the experimental X-ray structure. The calculated Ru–Cl distances are 0.006 Å short, on average. The calculated Cl–Ru–Cl angle is 0.9° too small, and the N–Ru–N angles are 4.1° and 5.1° too large. The Ru–N distances range from being 0.034 Å too short to being 0.015 Å too long (using a bond order of $^3/_2$). Since ruthenium is a low-spin d^6 ion in this complex, a bond order of $^3/_2$ is appropriate due to back-bonding involving the C–N π^* orbitals.[40]

***mer*-Trichloro[*N*-(3-aminopropyl)-1,3-diaminopropane]cobalt(III).**[41] The structure has been analyzed crystallographically and shows that the triamine chelate is bonded with the primary

(34) Steinfink, H.; Post, B.; Fankuchen, I. *Acta Crystallogr.* **1955**, *8*, 420.
(35) Haas, A.; Kutsch, H. J.; Krüger, C. *Chem. Ber.* **1987**, *120*, 1045.
(36) Dräger, V. M.; Mathiasch, B.; Ross, L.; Ross, M. *Z. Anorg. Allg. Chem.* **1983**, *506*, 99.
(37) Ghotra, J. S.; Hursthouse, M. B.; Welch, A. J. *J. Chem. Soc., Chem. Commun.* **1973**, *7*, 669.
(38) Sato, M.; Kosaka, M.; Watabe, M. *Bull. Chem. Soc. Jpn.* **1985**, *58*, 874.
(39) Pank, V.; Klaus, J.; von Deuten, K.; Feigel, M.; Bruder, H.; Dieck, H. *Trans. Met. Chem.* **1981**, *6*, 185.
(40) Shriver, D. F.; Atkins, P. W.; Langford, C. H. *Inorganic Chemistry*; W. H. Freeman: New York, 1990.
(41) Barefield, E. K.; Carrier, A. M.; Vanderveer, D. G. *Inorg. Chim. Acta* **1980**, *42*, 271.

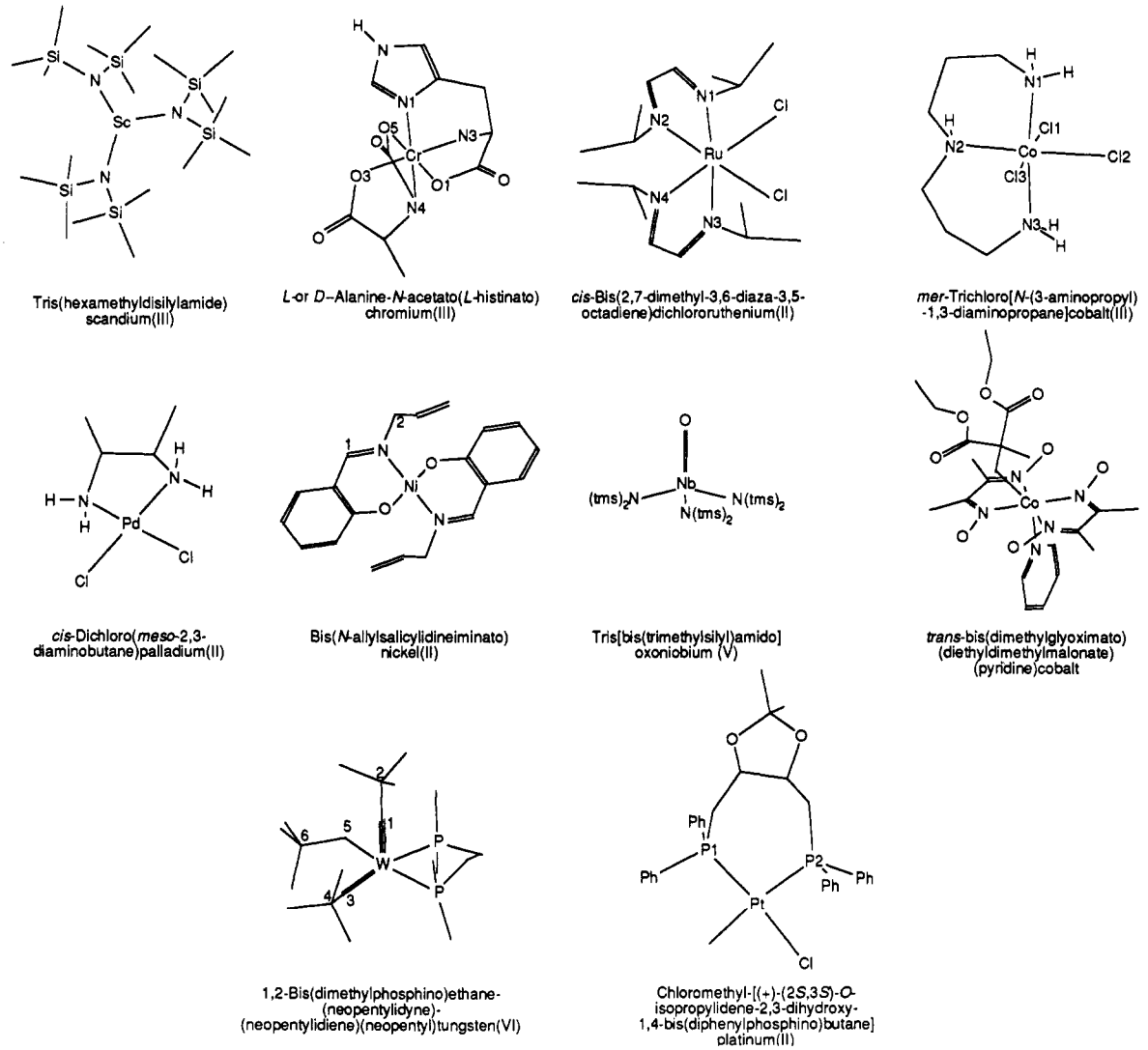

Figure 9. Structural formulas and numbering of atoms for a set of metal containing molecules.

amino groups trans. Overall, the experimental structure is well reproduced by UFF. The calculated Co–N distances are in very good agreement with experiment (errors within 0.011 Å). The calculated axial Co–Cl distances are 0.012 Å and 0.039 Å too short. The calculated equatorial Co–Cl bond (trans to nitrogen) is 0.078 Å too short, owing to an unaccounted for trans influence. The bond angles at Co are well reproduced by the force field.

***cis*-Dichloro(*meso*-2,3-diaminobutane)palladium(II).**[42] Structural studies of this complex show square-planar coordination. Two chlorine atoms are in cis postions, and the diamino ligand occupies two cis postions. The calculated results are in good to fair agreement with the experimental structure. The calculated Pd–Cl distances are only 0.003 Å too small. The Pd–N distances are 0.021 Å too small. The N–C distances are 0.040 Å too short. The small experimental angular distortion away from strict square planarity is underestimated by approximately 5° with the UFF force field.

Bis(*N*-allylsalicylidineiminato)nickel(II).[43] X-ray studies have shown that this Schiff base complex is nearly planar. The immediate coordination environment at Ni is calculated by UFF to be nearly planar, but significant distortions from planarity are observed in the next nearest neighbors. The calculated Ni–O bond is 0.039 Å short, and the Ni–N bond is 0.063 Å short. The computed C–O distance in the chelate ring is 0.011 Å long; the N–C imine distance is 0.023 Å long; and the N–C amine distance is 0.042 Å short. The intrachelate N–Ni–O bond angle is 2.1° small; the interchelate angle is 2° too large. The C, N, and O atoms of the salicylidineiminato ligands are described with resonating atom types and internal bond orders of $^3/_2$. The bonds to Ni use bond order 1.

Tris[bis(trimethylsilyl)amido]oxoniobium(V).[44] X-ray studies have shown that the coordination environment of the Nb is a distorted tetrahedron, with planar nitrogen atoms. The calculated O–Nb–N angle is 2.6° too large. The calculated N–Nb–N angle is 1.9° too small. The Nb–O bond distance (bond order 3) is well-predicted. The calculated Nb–N amide bond distances are 0.005 Å too long (bond order $^3/_2$), and the calculated Si–N bond distances are 0.051 Å too long.

Methylmanganese Pentacarbonyl.[45] The Mn–C distance for the metal–methyl bond is 0.054 Å short by UFF and the Mn–C distance for the equatorial metal–carbonyl bonds are only 0.009 Å long (bond order 2).

***trans*-Bis(dimethylglyoximato)(diethyl dimethylmalonate)-(pyridine)cobalt.**[46] X-ray studies of this cobaloxime have been carried out. The calculated structural parameters are in fair agreement with the experimental results. The calculated glyox-

(42) Ito, T.; Marumo, F.; Saito, Y. *Acta Crystallogr., Sect. B: Struct. Sci.* **1971**, *B27*, 1695.
(43) Bhatia, S. C.; Bindlish, J. M.; Saini, A. R.; Jain, P. C. *J. Chem. Soc., Dalton Trans.* **1980**, *7*, 1773.
(44) Hubert-Pfalzgraf, L. G.; Tsunoda, M.; LeBorgne, G. *J. Chem. Soc., Dalton Trans.* **1988**, 533.
(45) Hellwege, K-H. *Landolt-Bornstein Numerical Data and Functional Relationships in Science and Technology*; Springer Verlag: Berlin, 1976; Vol. 7, p 325.
(46) Randaccio, L.; Bresciani-Pahor, N.; Orbell, J. D.; Calligaris, M. *Organometallics* **1985**, *4*, 469.

imato Co–N distances are 0.043 Å long on average. The calculated pyridine Co–N distance is 0.119 Å short, consistent with a significant trans influence from the alkyl group (if a bond order of $^1/_2$ is used, the calculated pyridine Co–N distance is 0.047 Å long). The Co–C distance is only 0.023 Å long.

1,2-Bis(dimethylphosphino)ethane(neopentylidyne)(neopentylidene)(neopentyl)tungsten(VI).[47] X-ray studies have shown that the coordination environment of the W is a distorted square pyramid. The experimental distortion of the square pyramid plane away from tungsten is not accounted for in the present force field because an octahedral atom type is used for tungsten (W_6+6). Large angular errors at W result: the UFF C1–W–C3 angle is too small by 8°, the C1–W–C5 is too small by 20°. The experimental M–C single, double, and triple bond distances are well reproduced for this unique complex. This is a remarkable result considering a single covalent W radius is used in the UFF force field; the bond order correction can correctly account for the change in bond distance as a function of bond order. The W–C single bond is 0.05 Å short, the W–C double bond is 0.027 Å long, and the W–C triple bond is 0.029 Å long. The electronic effect at metal alkylidene centers whereby the M–C–C angle is enlarged as a result of a electronic donation from the α C–H bond to the metal center is not accounted for in the UFF force field, and hence the W–C_6–C_7 bond angle is 17° too small. The W–C–C angles for the W–C single and triple bonds are in error by less than 1°.

Chloromethyl[(+)-(2*S*,3*S*)-*O*-isopropylidene-2,3-dihydroxy-1,4-bis(diphenylphosphino)butane]platinum(II).[48] The structure of this complex has been analyzed crystallographically and the coordination of the platinum is essentially square planar. The two Pt–P bond distances are significantly different, consistent with trans-influence arguments. The Pt–P1 (trans to C1) is 0.007 Å short, bond order 2. The computed Pt–P2 (trans to carbon) distance is only 0.005 Å short, bond order $1^1/_2$. The calculated Pt–C and Pt–Cl distances are only 0.04 Å short and long, respectively.

(47) Churchill, M. R.; Youngs, W. J. *Inorg. Chem.* **1979**, *18*, 2454.
(48) Payne, N. C.; Stephan, D. W. *J. Organomet. Chem.* **1982**, *228*, 203.

IV. Conclusions

It is possible to construct a force field from simple rules and atomic parameters that is capable of reproducing most structural features across the periodic table with errors less than 0.1 Å in bond distances and 5° to 10° in angle bend. Further applications of UFF to organic, main group, and metal compounds are described in the following papers. Enhancements to UFF to decrease structural and energetic errors are underway.

Acknowledgment. A.K.R. gratefully acknowledges support of this research by Shell Development and Molecular Simulations Inc. W.A.G. gratefully acknowledges support of this research by a grant from DOE-AICD. A.K.R. and C.J.C. thank M.A.C. for her timely arrival and Glynis Hubbard for her contributions to this work.

Registry No. Octamethylcyclotetrasiloxane, 556-67-2; 1,3,5,7-tetrakis(trifluoromethyl)-2,4,6,8,9,10-hexathia-1,3,5,7-tetragermaadamantane, 108009-38-7; dodecaphenylcyclohexastannane, 1066-22-4; tris(hexamethyldisilylamide)scandium(III), 37512-28-0; (L- or D-alanine-*N*-acetato)(L-histidinato)chromium(III), 96126-28-2; bis(*N*-allylsalicylidineiminato)nickel(II), 55292-18-7; 1,2-bis(dimethylphosphino)ethane(neopentylidyne)(neopentylidene)(neopentyl)tungsten(VI), 70878-65-8.

Supplementary Material Available: Tables of reference compounds used to obtain covalent radii for main group and transition elements (8 pages). Ordering information is given on any current masthead page.

Application of a Universal Force Field to Organic Molecules

C. J. Casewit,*,† K. S. Colwell,‡ and A. K. Rappé*,‡

Contribution from Calleo Scientific, 1300 Miramont Drive, Fort Collins, Colorado 80524, and Department of Chemistry, Colorado State University, Fort Collins, Colorado 80523.
Received March 23, 1992

Abstract: The application of a Universal force field (UFF) to the treatment of organic molecules is described. The ability of the force field to predict the structures of a variety of organic molecules is examined, and the results are compared with the MM2 or MM3 force fields. UFF correctly predicts the structures of unstrained and uncongested hydrocarbons, silanes, alkenes, saturated amines, saturated ethers and phosphines, aromatic systems, and simple unconjugated multiple bond containing compounds such as nitriles, ketones, and imines well. Bond angles are usually correct to within 3°, and bond lengths usually to within 0.02 Å. Specifically, the rms error in the UFF predicted C–C bond distances is 0.021 Å, with a maximum of 0.067 Å for a set of 65 distances. For comparison, the MM2/3 RMS error in C–C distances is 0.012 Å with a maximum of 0.029 for the same set of molecules. The UFF rms error in C–N bond distances is 0.024 Å, with a maximum of 0.041 Å for a set of 13 distances. For the same set of molecules, the MM2/3 rms error in C–N distances is 0.013 Å with a maximum of 0.031. The UFF rms error in C–O bond distances is 0.025 Å, with a maximum of 0.05 Å for a set of seven distances. For the same set of molecules the MM2/3 rms error in C–O distances is 0.007 Å with a maximum of 0.015. The ability of UFF to calculate conformational energy differences in simple organic molecules is also examined.

I. Introduction

Over the last two decades, molecular mechanics has developed into a powerful and standard method for studying the molecular structure and related properties of organic molecules. The MM2,[1] MMP2,[2] MM3[3] force fields, developed by Allinger and his group, are the premier force fields for the prediction of organic structures and energies; the molecular mechanics results are usually of experimental accuracy. However, as pointed out in the first paper of this series,[4] standard force fields such as MM2 are limited to

† Calleo Scientific.
‡ Colorado State University.

(1) Allinger, N. L. *J. Am. Chem. Soc.* **1977**, *99*, 8127.
(2) Sprague, J. T.; Tai, J. C.; Yuh, Y.; Allinger, N. L. *J. Comput. Chem.* **1987**, *8*, 581.
(3) Allinger, N. L.; Yuh, Y. H.; Lii, J.-H. *J. Am. Chem. Soc.* **1989**, *111*, 8551.

0002-7863/92/1514-10035$03.00/0